Development 139, 2999-3009 (2012) doi:10.1242/dev.077800

Fascin controls neuronal class-specific dendrite arbor morphology

Julia Nagel[1,*], Caroline Delandre[2], Yun Zhang[1,*], Friedrich Förstner[3], Adrian W. Moore[2] and Gaia Tavosanis[1,*,‡]

SUMMARY

The branched morphology of dendrites represents a functional hallmark of distinct neuronal types. Nonetheless, how diverse neuronal class-specific dendrite branches are generated is not understood. We investigated specific classes of sensory neurons of *Drosophila* larvae to address the fundamental mechanisms underlying the formation of distinct branch types. We addressed the function of fascin, a conserved actin-bundling protein involved in filopodium formation, in class III and class IV sensory neurons. We found that the terminal branchlets of different classes of neurons have distinctive dynamics and are formed on the basis of molecularly separable mechanisms; in particular, class III neurons require fascin for terminal branching whereas class IV neurons do not. In class III neurons, fascin controls the formation and dynamics of terminal branchlets. Previous studies have shown that transcription factor combinations define dendrite patterns; we find that fascin represents a downstream component of such programs, as it is a major effector of the transcription factor Cut in defining class III-specific dendrite morphology. Furthermore, fascin defines the morphological distinction between class III and class IV neurons. In fact, loss of fascin function leads to a partial conversion of class III neurons to class IV characteristics, while the reverse effect is obtained by fascin overexpression in class IV neurons. We propose that dedicated molecular mechanisms underlie the formation and dynamics of distinct dendrite branch types to elicit the accurate establishment of neuronal circuits.

KEY WORDS: Fascin, Singed, Dendrite, *Drosophila*

INTRODUCTION

The function of neuronal circuits relies on establishing of the correct morphology of neurons. In particular, the morphology of the neuronal dendrite tree underlies both the formation of appropriate connections and accurate input processing (Branco et al., 2010; Häusser et al., 2000). The relevant morphological characteristics of dendrites, including their length, thickness and branching level, thus represent a functional hallmark of each neuronal type. But how the specific morphologies of dendrites of distinct neuronal classes are formed remains to be elucidated. A fundamental question in this context is whether the formation of specific branch types relies on molecularly separable mechanisms.

The morphology of dendrites is defined by transcriptional codes (Jan and Jan, 2010). For example, in the rodent cortex, the bHLH transcription factor neurogenin 2, which is involved in the specification of neuronal subtypes, defines the unipolar dendritic morphology of pyramidal neurons (Hand et al., 2005). In *Drosophila*, candidate-prompted analysis as well as large-scale screens have led to the identification of a number of transcription factors that are capable of modulating the morphology of peripheral nervous system (PNS) dendrites (Crozatier and Vincent, 2008; Grueber et al., 2003a; Hattori et al., 2007; Jinushi-Nakao et al., 2007; Li et al., 2004; Moore et al., 2002; Parrish et al., 2006; Sugimura et al., 2004). The identification of these transcription factor programs has revealed part of the developmental logic used to create neuron class-specific dendrite shape; yet the molecular programs that translate this logic into the branching and dynamic properties of each neuronal type remain unknown.

A subset of sensory neurons of the embryonic and larval PNS of *Drosophila* (da neurons) display complex dendrite morphology and can be separated into four morphological and functional classes. They represent a powerful system with which to investigate how class-specific neuron morphology is controlled (Grueber et al., 2002). Among da neurons, the most complex dendrites are displayed by class III and class IV neurons. Only class IV neurons have space-filling dendrites that branch extensively to cover to a great extent their receptive area. By contrast, the dendrites of class III neurons are decorated with actin-rich filopodia-like terminal branchlets called ‘spiked protrusions’. In the present work, we ask which effectors are involved in the distinction between class III and class IV morphology.

Both class III and class IV neurons express high levels of the atypical homeodomain-containing transcription factor Cut, although the level of expression in class III neurons is higher than in class IV. High-level Cut expression is necessary and sufficient to promote dendrite complexity and the formation of spiked protrusions (Grueber et al., 2003a). The different morphology of class IV neurons is obtained through lower levels of Cut protein combined with the expression of an additional transcription factor, Knot (Collier), which promotes microtubule-based dendrite extension (Crozatier and Vincent, 2008; Hattori et al., 2007; Jinushi-Nakao et al., 2007). At the level of an individual branch, however, what molecular mechanisms define the specific class III morphology, including the spiked protrusions?

[1]Dendrite Differentiation Group, Department of Molecular Neurobiology, MPI of Neurobiology, 82152 Munich-Martinsried, Germany. [2]Disease Mechanism Research Core, RIKEN Brain Science Institute, 2-1 Hirosawa, Wako-shi, Saitama, 351-0198, Japan. [3]Department of Systems and Computational Neurobiology, MPI of Neurobiology, 82152 Munich-Martinsried, Germany.

*Present address: Dendrite Differentiation Group, German Center for Neurodegenerative Diseases (DZNE), c/o Life and Medical Sciences (LiMeS), 53115 Bonn, Germany
‡Author for correspondence (gaia.tavosanis@dzne.de)

Accepted 1 June 2012

The production of a filopodium represents the initial step toward the formation of a dendrite branch (Heiman and Shaham, 2010). Filopodia are dynamic structures; their formation is achieved through actin polymerization and organization of the actin filaments into bundles (Faix et al., 2009; Mattila and Lappalainen, 2008). The stiffness required to power membrane protrusion is generated by bundling of filopodial actin filaments into tightly ordered unipolar bundles mediated by the conserved protein fascin (Vignjevic et al., 2006), which contains two actin-binding sites (Ono et al., 1997; Sedeh et al., 2010; Yamakita et al., 1996). In *Drosophila*, the only gene encoding fascin is *singed* (*sn*). Mutations in *singed* perturb a number of actin-dependent processes, including the formation of adult fly bristles, the motility of blood cells and the formation of an oocyte (Cant et al., 1994; Tilney et al., 1998; Wulfkuhle et al., 1998; Zanet et al., 2009).

Here, we have investigated whether fascin has a generalized role in branch formation in *Drosophila* larval da neurons. We have quantitatively described the morphological distinction between class III and class IV terminal branching in larval da neurons and have analyzed the distinctive dynamic properties of their terminal branchlets. In contrast to expectations, we found that fascin is not involved, in general, in the formation of dendrite branches, but rather in the formation of a very specific type of branch: the class III neuron spiked protrusion. Furthermore, we show that fascin is an effector of Cut, the principal transcription factor that controls class III neuron morphology. Finally, our loss- and gain-of-function experiments indicate that fascin is a key factor in defining the morphological distinction between class III and class IV neurons.

MATERIALS AND METHODS

Genetics and fly lines

sn^3 and *sn^{36a}* were as described (Cant et al., 1994; Paterson and O'Hare, 1991; Roiha et al., 1988). The following constructs were used: *80G2Gal4* (Gao et al., 1999), *c161Gal4* (Shepherd and Smith, 1996), *477Gal4* (Grueber et al., 2003a), *2-21Gal4 UASmCD8GFP* (Grueber et al., 2003a), *ppkEGFP* (Grueber et al., 2003b), *UAScutEHK* (Grueber et al., 2003a) and *UASrac1.L* (Luo et al., 1994). Genotypes are listed in supplementary material Table S1. For MARCM (Grueber et al., 2002), *sn^{36a}* was recombined with *FRT19A* and *tubGal80, hsFLP, FRT19A; 109(2)80Gal4 UASmCD8GFP/CyO* was crossed to *sn^{36a} FRT19A/Y* and *FRT19A*/Y. Third instar larvae were directly examined for mutant clones.

Molecular procedures

To generate fluorescently tagged Singed constructs we cloned the cDNA of Kushabira-Orange (mKO) or GFP from pmKO1-MN1 (MBL, Naka-ku Nagoya, Japan) and pRmHa3-GFP-actin (H. Oda, Osaka, Japan), respectively, into pUAST (Brand and Perrimon, 1993). *singed* cDNA (clone LD16477, BioCat, Heidelberg, Germany) was then cloned downstream of the fluorescent tags, including a spacer (5′-GGCGGCCGCGGA-3′). To generate the Singed phosphovariants, mKO-tagged Singed was subcloned into pUASTattB (Bischof et al., 2007). Site-directed mutagenesis on Ser52 was performed by PCR (Stratagene Quick Change Site-Directed Mutagenesis Kit). To achieve comparable levels of expression, all constructs were inserted into the *51D attP* landing site (Bischof et al., 2007). All constructs were verified by sequencing.

Immunohistochemistry

Filleted and fixed wandering third instar larvae (Grueber et al., 2002) were probed with mouse anti-Singed 7C (1:20; Development Studies Hybridoma Bank, Iowa City, IA, USA) and rabbit anti-GFP (1:1000; Living Colors) antibodies, followed by secondary antibodies (Jackson). The larva filets were analyzed by confocal microscopy (Leica TCS SP2) using a 40× objective. Futsch labeling was performed as described (Yalgin et al., 2011).

Time-lapse and imaging

Living wandering third instar larvae were immobilized by pressure and imaged with a Leica TCS SP2 confocal microscope. For time-lapse imaging of dendrite dynamics, second instar larvae (~48 hours after egg laying) were not anesthetized, but immobilized with an air-permeable sieve (Dimitrova et al., 2008). Confocal stacks (six images spaced by 1.6 μm) were acquired every 5 minutes over a period of 30 minutes with a 40× objective. For two-color time-lapse imaging, *UAS-GFPsn/+; c161Gal4 UASmCD8cherry/+* larvae were anesthetized in ether (Zito et al., 1999) and imaged with a spinning disc confocal microscope [CSU10 Real-Time Confocal System (Visitron Systems, Germany) on a Zeiss Observer 1 microscope] with a Photometrics CoolSNAP HQ2 camera. Confocal stacks (ten slices spaced at 1 μm intervals) were taken every 3 minutes over a period of 15 minutes with a 63× objective. Single time points were deleted if the larva moved.

Image analysis and statistics

Images were analyzed with ImageJ software (NIH), using the NeuronJ plug-in (Meijering et al., 2004) to trace the dendritic branches. In class III neurons, spiked protrusions were defined as unbranched terminal processes shorter than 30 μm. To analyze the branch distribution in class IV neurons we used Sholl analysis (Sholl, 1953) (ImageJ). For time-lapse analysis, every time point was analyzed separately. At least five animals per genotype were used for quantification. To measure the curviness of terminal branchlets we calculated convex hulls (supplementary material Fig. S1A). This method is rather insensitive to curvature changes of short branches owing to minor reconstruction artifacts after optical imaging and includes both a linear and a curvature component (supplementary material Fig. S1B,C). To calculate the convex hulls, NeuronJ traces were reconstructed to vectorized directed binary tree structures using the TREES toolbox (Cuntz et al., 2010). Convex hulls were computed using built-in MATLAB (MathWorks) functions. Two-color time-lapse movies were analyzed using ImageJ. The spiked protrusion area was defined by thresholding and manually selected. The average signal intensity of GFP-Singed was normalized over that of membrane-bound mCD8-cherry in the defined spiked protrusion area. In total, 176 extension or retraction events from four different animals were analyzed.

Statistical analysis was performed using Student's *t*-test for comparing two groups. For more than two groups, one-way ANOVA and a Bonferroni's multiple comparison test for normally distributed samples and Dunn's multiple comparison test for non-normally distributed samples were used.

RESULTS

Distinctive properties of terminal branchlets in class III and class IV neurons

We analyzed the distinction between two neuronal types in the *Drosophila* larval PNS: the class III and class IV da neurons (Fig. 1A,B). These are the most complex da neurons, they both express the transcription factor Cut at relatively high levels, they largely overlap and are likely to share a similar milieu.

In agreement with previous results, we found that class IV dendrites are more extended and more complex as judged by their higher dendrite branch order and number of dendrite termini (data not shown) (Grueber et al., 2002). In addition, the filopodia-like terminal branchlets represent a most distinctive feature of class III and class IV neurons. We evaluated the difference between the filopodia-like terminal branchlets of the two neuronal types using an algorithm that accurately describes the morphological properties of a neuron (Cuntz et al., 2010). The characteristic terminal branchlets of class III neurons are called spiked protrusions (Grueber et al., 2002). They were short (5 μm on average) and straight (Fig. 1C-F). By contrast, the terminal branchlets of class IV neurons were longer (15 μm on average) and often bent (Fig. 1C,G-I). We quantified the curvature differences between these two

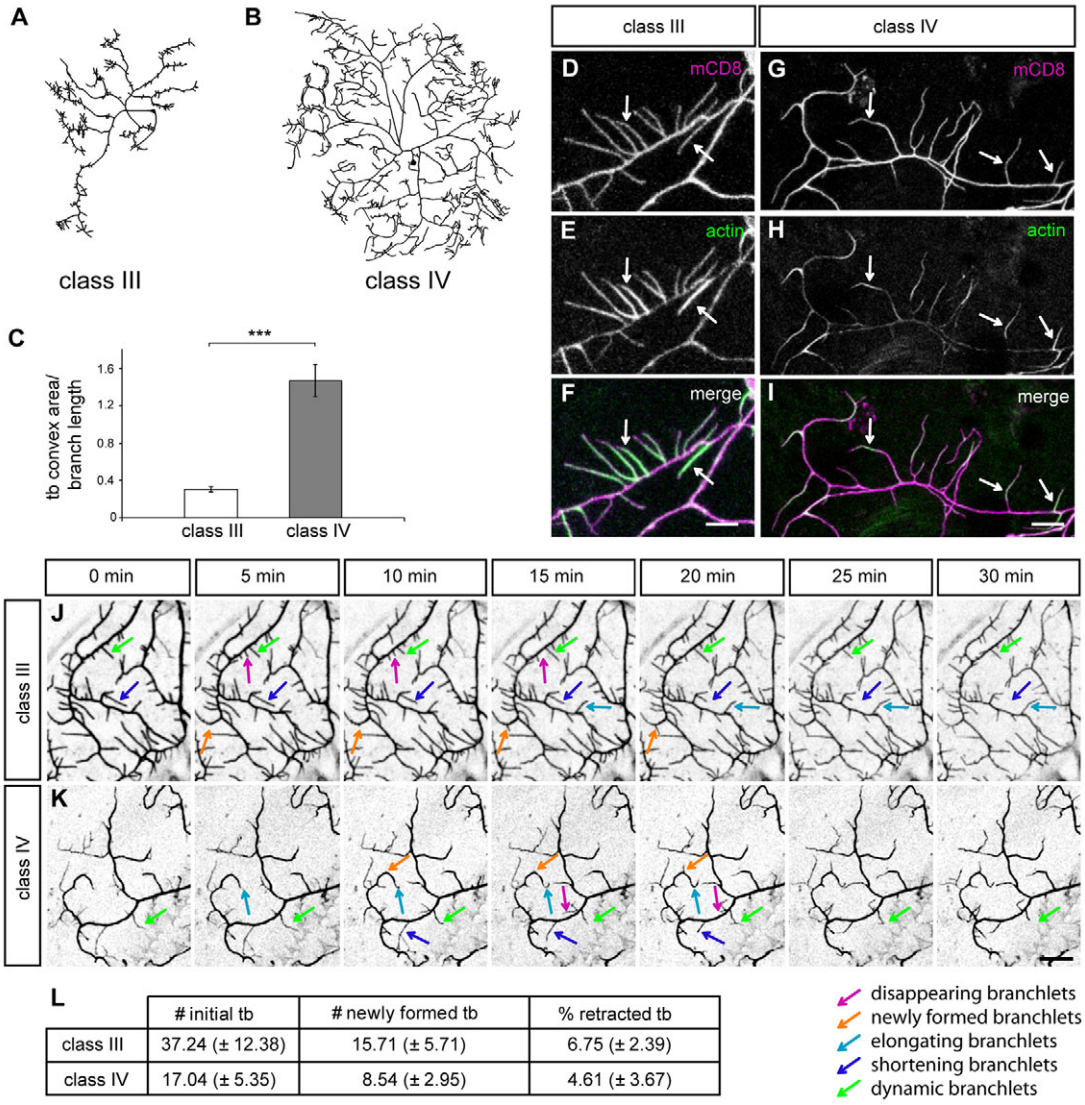

	# initial tb	# newly formed tb	% retracted tb
class III	37.24 (± 12.38)	15.71 (± 5.71)	6.75 (± 2.39)
class IV	17.04 (± 5.35)	8.54 (± 2.95)	4.61 (± 3.67)

Fig. 1. Distinctive properties of terminal branchlets of class III and class IV neurons. (**A**,**B**) Tracings of a class III ldaB neuron (A) and of a class IV ddaC neuron (B). (**C**) Class III neuron terminal branchlets have a significantly smaller convex area/branch length than class IV neurons. ***P<0.001; error bars indicate s.d. (**D-I**) Actin localization in terminal branchlets of class III (D-F) and class IV (G-I) neurons in third instar larvae. (D-F) Actin-GFP localizes to the terminal branchlets of class III neurons, mainly along their whole length (arrows). (G-I) Actin-GFP localizes to terminal branchlets of class IV neurons, mainly within defined subdomains (arrows). (**J**,**K**) Time-lapse imaging of terminal branchlets of class III ldaB (J) and class IV ddaC (K) neurons in second instar larvae (*c161Gal4 UASmCD8GFP* and *ppkeGFP*, respectively). Stacks were taken every 5 minutes over a 30-minute period and maximal projections of each stack are shown. (**L**) The number of terminal branchlets and the number of newly formed branchlets per 100 μm branch length are significantly higher in class III than in class IV neurons. The percentage of retracted branchlets is similar in both classes. Values are ± s.d. See also supplementary material Fig. S1 and Movies 1 and 2. tb, terminal branch. Scale bars: 5 μm in D-F; 10 μm in G-K.

branching types, based on the convex hull spanned by a terminal branchlet (see Materials and methods and supplementary material Fig. S1). The area of a convex hull, normalized to the branchlet length, was significantly larger in class IV than in class III neurons, indicating that the terminal branchlets are significantly more curved in class IV than in class III neurons (Fig. 1C).

The cytoskeletal organization is also different between class III and IV terminal branchlets (Fig. 1D-I). Actin is enriched in the terminal processes of both neuronal types. A large fraction of the terminal branchlets of class III neurons was completely filled with actin-GFP, as previously reported (Andersen et al., 2005; Li et al., 2005; Medina et al., 2006; Medina et al., 2008) (Fig. 1D-F). By contrast, in class IV neurons actin was discontinuous and enriched within subdomains of longer branchlets. Only a few shorter branchlets were completely decorated (Fig. 1G-I). Tubulin did not invade the terminal branchlets of either neuronal type as judged by tubulin-GFP localization and immunodetection of endogenous tubulin or of the MAP1B-like protein Futsch (Hummel et al., 2000) (data not shown).

To investigate the dynamics underlying this morphological and structural distinction, we carried out time-lapse analysis of the filopodia-like terminal branchlets of these two classes of neurons (Andersen et al., 2005; Dimitrova et al., 2008; Grueber et al., 2003b; Sugimura et al., 2003). Both neuronal classes had highly

dynamic terminal branches in second instar larvae that grew and retracted during the imaging time of 30 minutes (Fig. 1J-L; supplementary material Movies 1, 2) (Andersen et al., 2005; Dimitrova et al., 2008). There was still significant dynamics in third instar larvae (data not shown). Qualitatively, class III neuron spiked protrusions extended and retracted maintaining a similar trajectory, whereas class IV terminal branchlets changed their extension direction displaying a behavior that we define as 'exploratory'. The number of terminal branchlets per 100 μm dendrite length was higher in class III than in class IV neurons at the beginning of the recordings (37.24 versus 17.04; $P<0.05$). Also, the rate of new terminal branchlet formation was higher in class III than in class IV neurons (15.71 versus 8.54 per 100 μm in 30 minutes in class III versus class IV; $P<0.05$), but the percentage of branches that completely retracted during the imaging time was approximately the same in both neuronal types (6.75% versus 4.61% of initial branches per 100 μm in 30 minutes in class III versus class IV; $P>0.5$). These dynamics could explain the higher number of terminal branchlets in class III versus class IV neurons. All other parameters that we have quantified, including the fraction of stable and dynamic branchlets, showed no significant differences between the two neuronal classes.

Class III and class IV neurons thus display distinct high-order branches, with differing morphologies, cytoskeletal organization and dynamics.

Fascin is enriched in class III da neuron terminal branchlets

Next, we addressed whether distinct molecules are involved in the formation and dynamics of terminal branches in these two neuronal classes. Following an RNAi-based screen (to be described elsewhere) in which we tested conserved actin-regulatory factors, we identified fascin (Singed) as a potential candidate. We analyzed the localization of Singed with monoclonal anti-Singed antibodies during the formation of high-order branches of da neurons, a process that might require filopodium formation. In third instar larva filets, Singed was enriched in class III neuron spiked protrusions in comparison to the main dendritic branches (Fig. 2A-C). This labeling was specific as it was no longer detectable in the sn^{36a} loss-of-function mutant (Cant et al., 1994) (Fig. 2D-F). By contrast, we could not detect a positive signal in dendrites of class I, II and IV neurons (Fig. 2G-I; data not shown). Importantly, the cell bodies of all da neurons were positively labeled, showing no obvious differences in the level of Singed signal between the different classes (Fig. 2B,H). These data suggest that Singed is present in all classes, but is differentially localized to terminal branches only in class III neurons.

The detection of endogenous Singed in da neurons might be partially obscured by its expression in surrounding tissue. For this reason, we generated a fluorescently tagged Singed construct (*mKOsn*) that produced a functional protein (supplementary material Fig. S2A-F). We expressed the construct at low levels in da neurons and revealed a very similar localization to that of the endogenous protein. Indeed, mKOSn was not enriched in particular dendritic subdomains in class I or IV neurons (Fig. 2M-R), although actin does accumulate in distinct regions within class IV neuron terminal branchlets (Fig. 1G-I). By contrast, mKOSn was specifically localized within the spiked protrusions of class III neurons (Fig. 2J-L). Hence, the localization of fluorescently tagged Singed recapitulates that of the endogenous protein. Although Singed was expressed in all da neurons, it was specifically enriched in class III spiked protrusions.

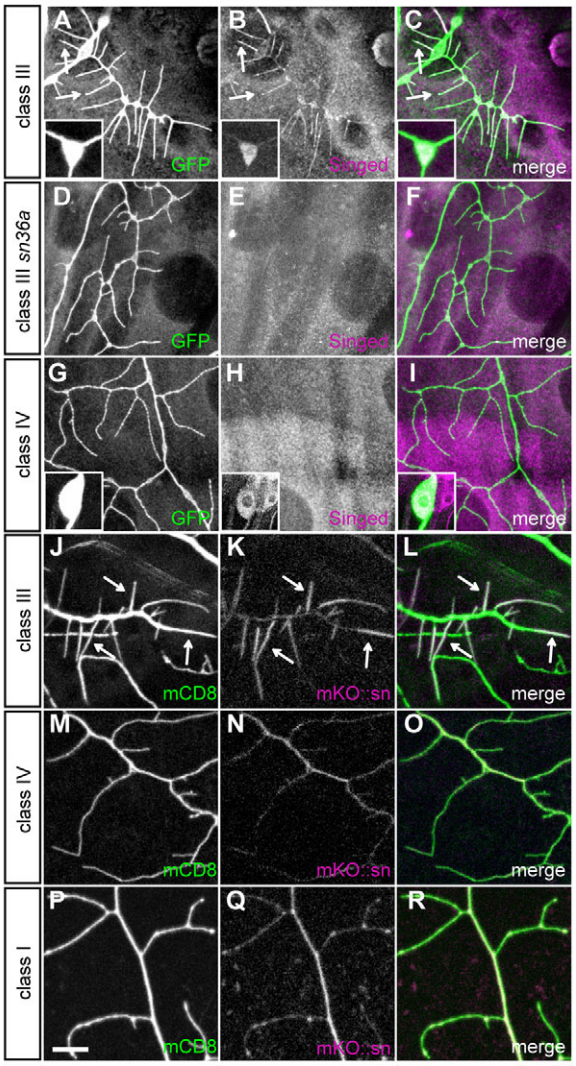

Fig. 2. Singed localizes to the spiked protrusions of class III neurons. (**A-F**) Endogenous Singed is enriched within the terminal branchlets in class III neurons (arrows). Wild-type (A-C) and sn^{36a} mutant (D-F) class III ldaB neurons of *c161Gal4 UASmCD8GFP* third instar larvae. Singed is barely or no longer detected in the sn^{36a} mutant. (**G-I**) In class IV ddaC neurons (*477Gal4; UASmCD8GFP*) endogenous Singed is detected within the cell body (inset), but not at the terminal branches. (**J-R**) Kushabira-Orange-tagged Singed (mKOsn) is enriched within the terminal branchlets of ddaA class III neurons (arrows) (*80G2Gal4 UASmKOsn*) (J-L), but shows no specific localization at terminal branches of ddaC class IV neurons (*477Gal4/UASmKOsn; UASmCD8GFP*) (M-O) or of ddaE class I neurons (*UASmKOsn/+; c161Gal4 UASmCD8GFP*) (P-R). There might be some enrichment at branching points. See also supplementary material Fig. S2. Scale bar: 10 μm.

Singed is required to form class III neuron spiked protrusions and to maintain their dynamics

The striking specificity of localization suggested that Singed might have a specific function in the class III neuron spiked protrusions. Therefore, we addressed the effect of *singed* mutations on class III neuron structure. The dendrites of class III ldaB neurons of third instar larvae are decorated with actin-rich spiked protrusions (Fig. 1D-F; number of protrusions, ±s.e.m., 238±29) at a density of 0.1/μm (Fig. 3A,A′,E,F). By contrast, in sn^{36a} loss-of-function

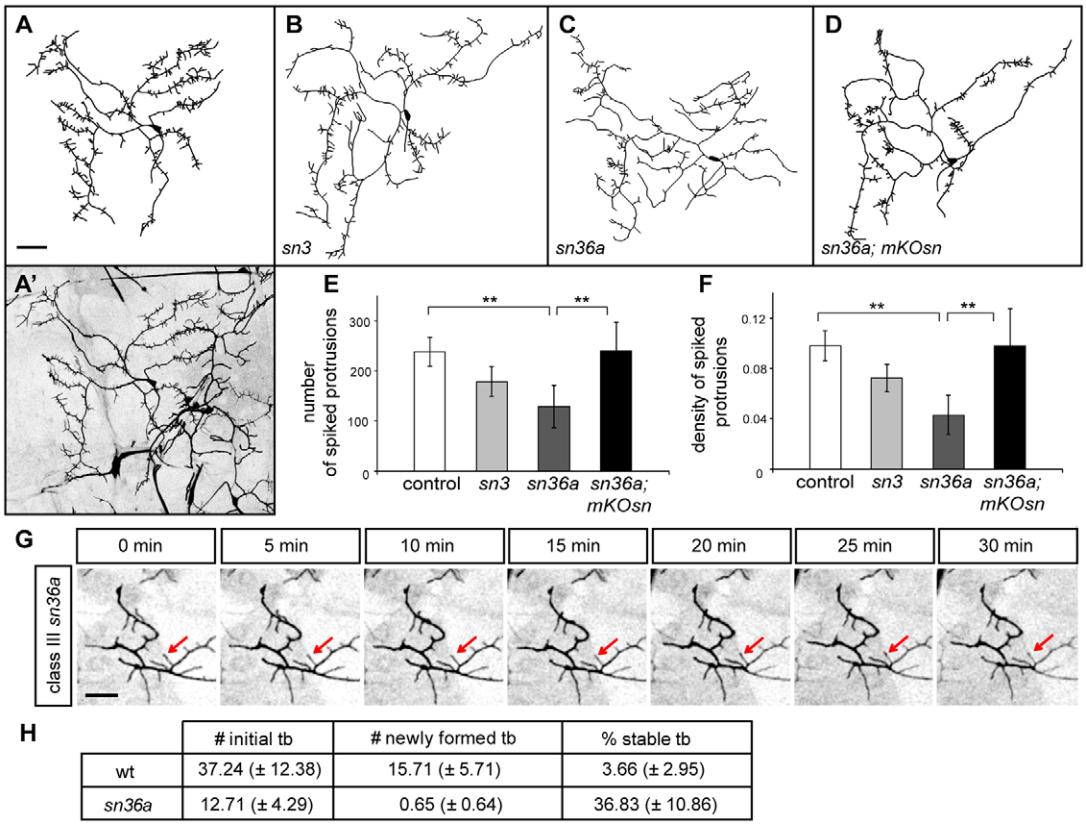

H

	# initial tb	# newly formed tb	% stable tb
wt	37.24 (± 12.38)	15.71 (± 5.71)	3.66 (± 2.95)
sn36a	12.71 (± 4.29)	0.65 (± 0.64)	36.83 (± 10.86)

Fig. 3. Loss of Singed leads to a decrease in spiked protrusion density and dynamics in class III neurons. (**A-D**) Tracings and original image (A′) of class III ldaB neurons of third instar wild type (A,A′), sn^{3} (B) and sn^{36a} (C) larvae expressing *mCD8GFP* under the control of *c161Gal4*. (D) Cell-autonomous rescue of the sn^{36a} mutant phenotype by expressing *mKOsn* in class III neurons. (**E**,**F**) The total number (E) and density (F) of spiked protrusions in class III ldaB neurons are significantly reduced in the sn^{36a} mutant and are rescued to wild-type levels by cell-autonomous expression of *mKOsn*. $^{**}P<0.01$; error bars indicate s.d. (**G**) Time-lapse imaging of terminal branchlets of sn^{36a} class III ldaB neurons of second instar larvae (*c161Gal4 UASmCD8GFP*). Arrow points to a branchlet that is not dynamic over the imaging time. Stacks were taken every 5 minutes over a 30-minute period and maximal projections of each stack are shown. (**H**) Terminal branchlet (tb) dynamics of wild-type and sn^{36a} class III neurons. The numbers of initial and of newly formed branchlets per 100 μm branch length are significantly reduced in sn^{36a} class III neurons. The fraction of stable branchlets is instead significantly increased in the sn^{36a} class III neurons. Values are ±s.d. See also supplementary material Fig. S3 and Movie 3. Scale bars: 50 μm in A-D; 10 μm in G.

mutants (Cant et al., 1994; Roiha et al., 1988) the number of spiked protrusions and their density were clearly reduced (number, 130±42; $P<0.01$; density, 0.04/μm; $P<0.01$; Fig. 3C,E,F). This was not due to a general defect in dendrite extension, as the total branch length of the dendritic tree was unaffected in *singed* mutant larvae (control, 3888±332 μm; sn^{36a}, 3981±575 μm; $P>0.5$). With the hypomorphic allele sn^{3} (Cant et al., 1994; Roiha et al., 1988) we obtained a similar, although less pronounced, phenotype (Fig. 3B,E,F). This phenotype was cell-autonomous, as it could be rescued upon expression of the functional fluorescently tagged Singed construct (*mKOsn*) using *c161Gal4*, a driver that allows for expression specifically in class I, II and III da neurons but not in epidermal or muscle cells (Shepherd and Smith, 1996). One copy of the *mKOsn* construct in a sn^{36a} background restored the number of spiked protrusions (240±56; $P>0.5$) and their density (0.1/μm of branch length; $P>0.5$) to control levels (Fig. 3D-F). In addition, we generated single-cell clones mutant for sn^{36a} with MARCM (mosaic analysis with a repressible cell marker) (Lee and Luo, 1999) and confirmed that the loss of actin-rich spiked protrusions is cell-autonomous in class III neurons (supplementary material Fig. S3). Thus, Singed acts cell-autonomously in the formation or maintenance of class III neuron spiked protrusions.

To distinguish between a defect in branchlet formation or maintenance, we carried out time-lapse analysis of terminal branchlets in sn^{36a} second instar larvae (Fig. 3G; supplementary material Movie 3). At this stage, sn^{36a} dendrites are already very different from those of control animals. First, we found that the total number of spiked protrusions at the beginning of the movies was lower in mutant than in control class III neurons (12.71/100 μm; $P<0.01$; Fig. 3H). Second, the rate of new branchlets formed was strikingly reduced (0.65; $P<0.01$; Fig. 3H). Moreover, the overall dynamics of the terminal branchlets was reduced. The number of existing branches that did not modify their length was increased 10-fold over that of the control (control, 3.66±2.95%; sn^{36a}, 36.83±10%; $P<0.01$; Fig. 3H) and the percentage of branchlets that disappeared, retracted or extended was significantly reduced. Hence, Singed is not only important for the formation of new spiked protrusions but also for maintaining their dynamics.

Singed is enriched in extending terminal branchlets of class III neurons

To address how Singed regulates class III terminal branchlet formation and dynamics, we analyzed the localization of fluorescently tagged Singed during branch formation, extension and

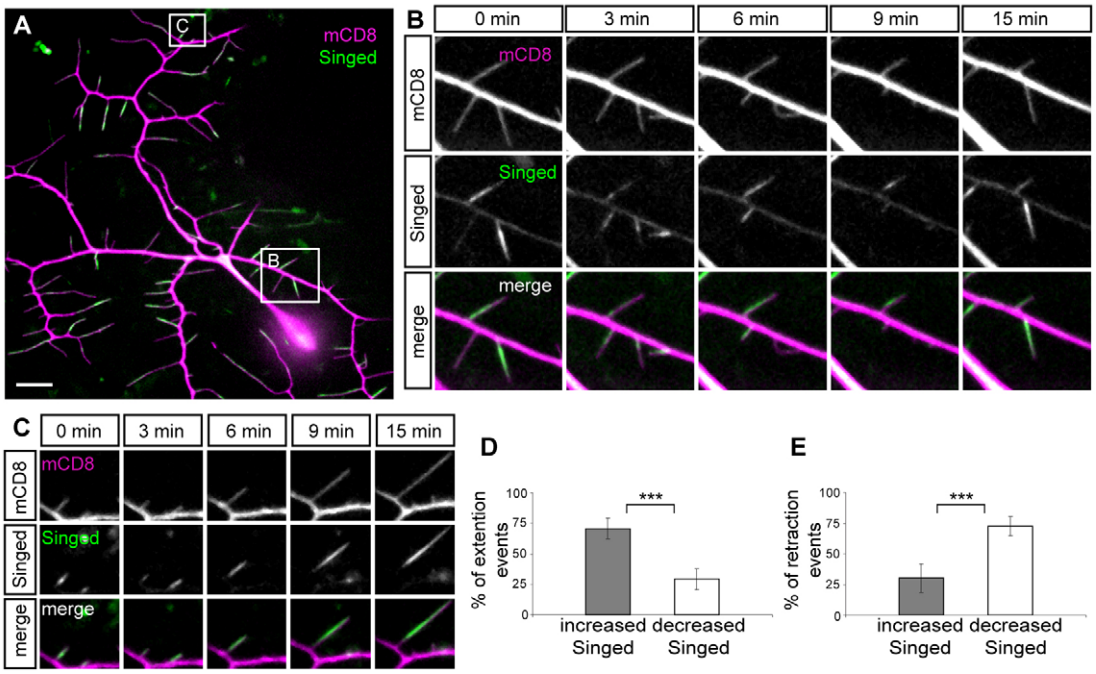

Fig. 4. Singed accumulates within extending terminal branchlets of class III neurons. Time-lapse analysis of Singed localization during terminal branchlet dynamics in class III neurons expressing membrane-tagged Cherry (mCD8) and GFP-Singed. (**A**) One of the imaged neurons at time point 0. (**B**,**C**) Time-lapse sequence of the regions boxed in A. (**D**,**E**) During extension events Singed preferentially accumulates from one time point to the next (D), whereas during most of the retraction events Singed levels decrease (E). ***P<0.001; error bars indicate s.d. See also supplementary material Movie 4.

retraction by time-lapse imaging (Fig. 4). We found a close correlation between the amount of Singed on a defined branchlet and its dynamic state. In fact, Singed accumulated on a large fraction of extending branches (71±9%; Fig. 4B-D). A significantly smaller fraction (29±9%; P<0.001) of the extending branchlets showed reduction in Singed levels (Fig. 4D). By contrast, only a small fraction of the retracting branchlets displayed Singed accumulation (30±12%; Fig. 4B,E) and in most of the retracting branchlets Singed signal was decreased (72±7%; P<0.001; Fig. 4B,E).

Taken together, Singed enrichment is a hallmark of extending branchlets and reduction of Singed signal correlates with retraction. The loss-of-function phenotype showed that Singed is involved in the maintenance of branchlet dynamics (Fig. 3G,H). Thus, it is conceivable that Singed accumulation promotes extension and that removal of Singed allows retraction.

Singed is necessary for Cut-dependent induction of spiked protrusions in class I neurons

High-level expression of the transcription factor Cut is necessary for the formation of class III spiked protrusions. In addition, Cut overexpression in simple class I neurons induces increased complexity and the formation of spiked protrusions, suggesting that high expression levels of Cut are sufficient to define class III morphology (Grueber et al., 2003a). Hence, we examined whether Singed might be an effector of Cut. When we overexpressed Cut in class I neurons using the *2-21Gal4* driver (Grueber et al., 2003a), this resulted, as expected, in an increase in dendrite complexity and in the formation of spiked protrusions (134±30 in Cut overexpression; there are no spiked protrusions in the control; Fig. 5C,C′) (Grueber et al., 2003a). Importantly, some of the ectopically formed spiked protrusions contained endogenous Singed (Fig. 5F-H′). This is in clear contrast to control class I neurons, in which neither endogenous nor overexpressed fluorescently tagged Singed was localized in defined dendrite domains (Fig. 2P-R). These data strongly suggest that Cut promotes Singed recruitment to the terminal branchlets.

Overexpression of Cut in class I neurons of sn^{36a} larvae led to an expansion of the dendrite tree that was even larger than in the wild-type background (Fig. 5D; supplementary material Fig. S4J,Q). In addition, the formation of ectopic spiked protrusions was clearly reduced by more than 40% (79±20; P<0.01; Fig. 5D-E), indicating that the formation of spiked protrusions through Cut requires Singed.

To address the nature of the expansion of the class I vpda neuron dendrites in these conditions, we investigated the proportion of dendrites positive for the microtubule-binding protein Futsch (Hummel et al., 2000). Loss of Singed contributes to an extension of the Futsch-positive domain of class I neuron dendrites overexpressing Cut (supplementary material Fig. S4N,O,Q). Thus, in addition to its role in shaping the actin-rich terminal branchlets, Singed also contributes to the restriction of microtubule-based dendrite extension.

Taken together, Singed is recruited to the Cut-induced spiked protrusions in class I neurons and is a downstream effector enabling Cut to induce spiked protrusion formation; it might also interact with Cut-driven morphogenesis programs in non-terminal branches.

Singed promotes class III versus class IV morphology

In addition to the reduction of class III spiked protrusions, the appearance of the remaining high-order processes of class III neurons was also altered in the *singed* mutants. First, in contrast to the short and straight wild-type spiked protrusions (Fig. 6A), class III neuron terminal branchlets were bent in the mutants (Fig. 6B). Indeed, the convex area spanned by the terminal branchlets was

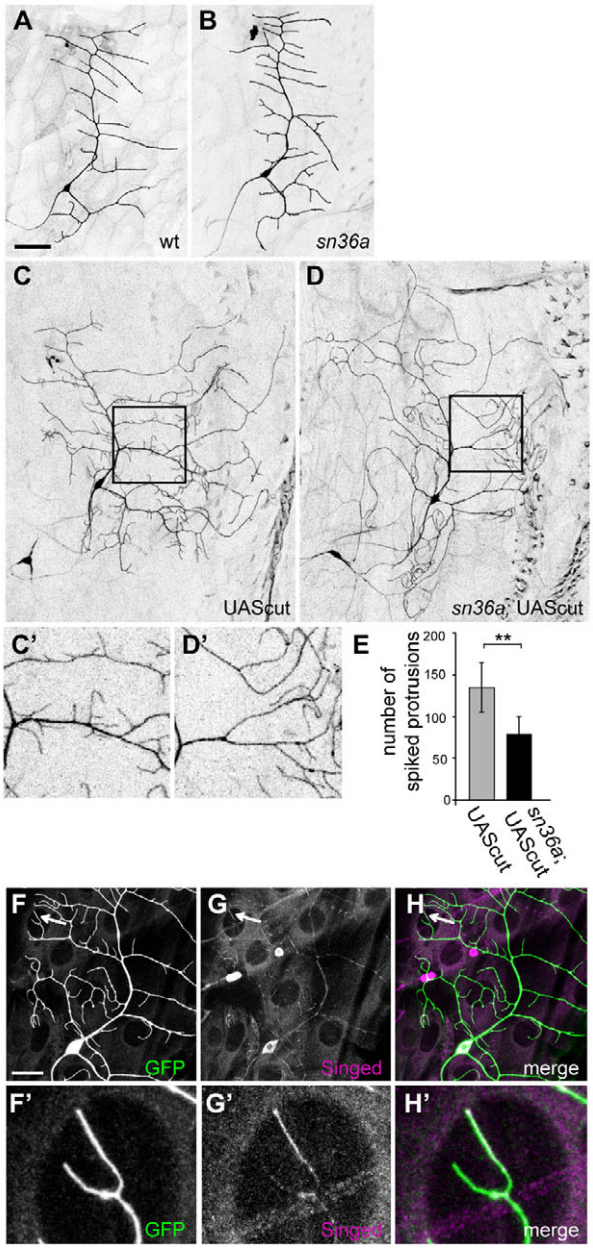

Fig. 5. Singed is essential for the formation of Cut-induced spiked protrusions. (**A-D'**) Class I vpda neurons (*2-21Gal4 UASmCD8GFP*) of (A) wild-type and (B) sn^{36a} third instar larvae. (C,D) Overexpression of the transcription factor *cut* in wild-type or in the sn^{36a} background. (C′,D′) Magnification of the boxed regions from C,D. (**E**) The number of ectopically formed short terminal branchlets upon *cut* overexpression in class I neurons is significantly reduced in the sn^{36a} background. $^{**}P<0.01$; error bars indicate s.d. (**F-H'**) Cut-overexpressing class I vpda neurons show localization of endogenous Singed at several ectopically formed terminal branchlets. (F′-H′) Magnification of the regions indicated by arrows in F-H. Scale bars: 50 μm in A; 25 μm in F.

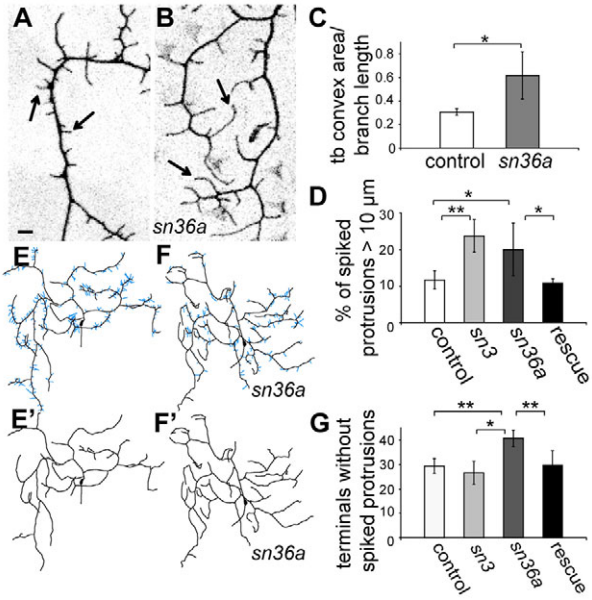

Fig. 6. Singed controls spiked protrusion length and arbor complexity. (**A**,**B**) Terminal branchlets of a wild-type (A) and a sn^{36a} (B) class III ldaB neuron (arrows). (**C**) Quantification of the curvature of terminal branchlets of class III ldaB neurons. (**D**) The percentage of spiked protrusions exceeding 10 μm is significantly increased in sn^{3} and sn^{36a} mutants. This phenotype is cell-autonomously rescued by *mKOsn* expression. (**E-F'**) Tracing of a wild-type (E) and a sn^{36a} (F) class III ldaB neuron; terminal branchlets that are shorter than 30 μm are indicated in blue. (E′,F′) The same tracings after eliminating the blue terminal branchlets. (**G**) The number of terminals left after pruning the terminal branchlets of less than 30 μm is significantly increased in the sn^{36a} mutant and can be rescued cell-autonomously. $^{*}P<0.05$; $^{**}P<0.01$; error bars indicate s.d. Scale bar: 10 μm.

clearly increased in the mutant (Fig. 6C). Interestingly, in the mutant this parameter lays between the values obtained in class III and class IV neurons, suggesting a partial shift of branchlet morphology toward that of class IV neurons (compare with Fig. 1C). In addition, the fraction of spiked protrusions exceeding 10 μm was 12±3% in the control, but increased to 20±8% in sn^{36a} ($P<0.05$) and to 24±5% in sn^{3} ($P<0.01$) mutants, and was restored to control levels upon cell-autonomous expression of *mKOsn* (11±2%; $P>0.5$) (Fig. 6D). Thus, this parameter too was shifted toward values typical of class IV neurons.

Second, not only were the number, density and morphology of the terminal branchlets modified, but also the overall tree complexity appeared slightly increased. For instance, the number of all termini, excluding the terminal branchlets of less than 30 μm (Fig. 6E′,F′,G), was significantly increased in mutant class III neurons (control, 29±3; sn^{36a}, 40±4; $P<0.01$; cell-autonomous rescue, 30±6; $P>0.5$) (Fig. 6G).

Thus, loss of Singed modified the number, density and morphology of the class III neuron terminal branchlets. In addition, it increased the complexity of the dendrite tree. Hence, these neurons appeared to partially shift toward class IV morphology. Consequently, we investigated the role of Singed in elaborating the class IV neuron dendrite tree. However, the branching of class IV ddaC neurons was unaffected in sn^{36a} mutants (supplementary material Fig. S5). Taken together, Singed is necessary in class III neurons for proper terminal branchlet formation and to define tree complexity, but is dispensable in class IV neurons.

Singed overexpression in class IV neurons induces spiked protrusion formation

Singed was detectable within the cell body of class IV neurons (Fig. 2G-I), but *singed* mutants did not display defects in class IV dendrite morphology (supplementary material Fig. S5). We thus

hypothesized that, in these neurons, Singed might not be activated or localized appropriately to induce spiked protrusion formation. To test this, we overexpressed wild-type Singed in class IV neurons using the *4-77Gal4* driver line (Grueber et al., 2003a) and one copy of the *mKOsn* construct inserted at a defined position in the fly genome, which results in high expression levels (Bischof et al., 2007). Class IV neurons overexpressing Singed formed terminal branchlets that resembled spiked protrusions in that they were short and straight (Fig. 7B). The convex area spanned by the terminal branchlets of class IV neurons overexpressing Singed was shifted toward class III values (Fig. 7M). Furthermore, the percentage of long terminal branchlets (>10 μm) was significantly decreased in class IV neurons overexpressing Singed (Fig. 7L). Strikingly, a fraction of the shorter terminal branchlets now accumulated Singed (Fig. 7H-J; compare with Fig. 2M-O). We conclude that high levels of Singed are sufficient to drive spiked protrusion formation in class IV neurons.

Singed activity is modulated by phosphorylation

We next addressed how Singed is regulated in class III neurons. Small GTPases of the Rho family, including Rac1, can activate fascin in vitro (Adams and Schwartz, 2000; Hashimoto et al., 2007; Parsons and Adams, 2008). Furthermore, overexpression of Rac1 can induce the formation of extra filopodia in class III neurons (Andersen et al., 2005; Lee et al., 2003) (supplementary material Fig. S6). Nonetheless, loss of *singed* function led to a non-significant reduction in the density of filopodia formed upon Rac1 overexpression (supplementary material Fig. S6D,E), indicating that there was no interaction between these two molecules. Thus, Singed promotes terminal branchlet formation in class III neurons independently of Rac1, suggesting that another control mechanism is acting in these neurons.

The actin-bundling capacity of Singed is negatively controlled by phosphorylation within the MARCKS homology domain (Ser52 in *Drosophila*) (Holthuis et al., 1994; Ono et al., 1997). To address

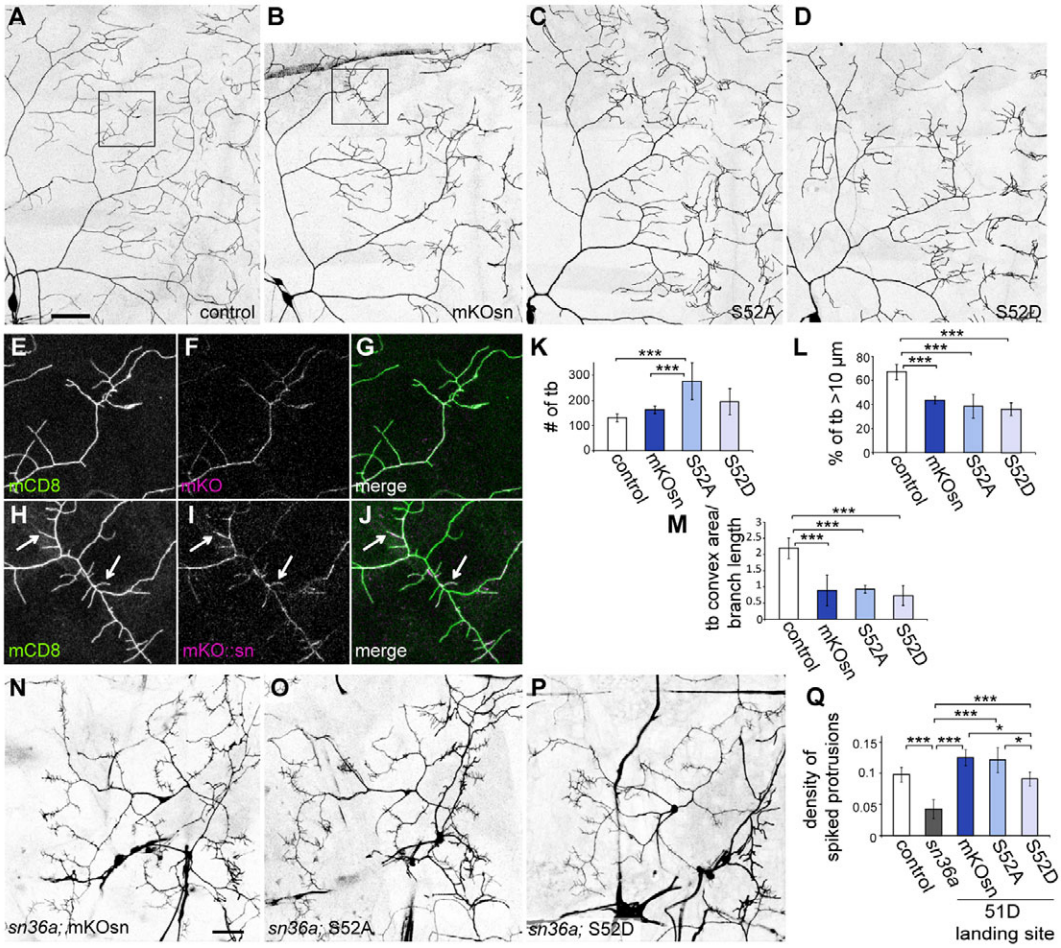

Fig. 7. Singed is sufficient to form spiked protrusions in class IV neurons upon overexpression and is partially regulated by phosphorylation. (**A-D**) Class IV ddaC neurons overexpressing the following constructs inserted at the *51D* landing site: (A) *mKO*, (B) *mKOsn*, (C) *mKOsnS52A* and (D) *mKOsnS52D*, together with *UASmCD8GFP*. The dorsal-posterior quarter of the dendritic tree is shown. (**E-G**) Kushabira-Orange (mKO) protein is uniformly distributed. (**H-J**) Strong overexpression of *mKOsn*, which leads to the formation of short terminal branchlets, is accompanied by recruitment of mKOsn to the ectopic short branchlets (arrows); compare with the absence of this enrichment at low expression levels that do not induce ectopic short branchlet formation (Fig. 2M-O). (**K**) Overexpression of *mKOSnS52A* induces significantly more terminal branches than *mKO* or *mKOsn*. (**L**) There is a significant decrease in terminal branches exceeding 10 μm upon overexpression of *mKOsn*, *mKOsnS52A* and *mKOsnS52D*. (**M**) Overexpression of *mKOsn*, *mKOsnS52A* and *mKOsnS52D* straightens the terminal branchlets significantly compared with *mKO*. See also supplementary material Figs S4 and S5. (**N-P**) Rescue of the spiked protrusion density phenotype of sn^{36a} class III ldaB neurons with (N) *mKOsn*, (O) *mKOsnS52A* and (P) *mKOsnS52D* at *51D* expressed with *c161Gal4*. (**Q**) Quantification of the density of spiked protrusions in sn^{36a} mutants, which is rescued by *mKOsn*, *mKOsnS52A* and *mKOsnS52D* constructs. However, *mKOsnS52D* yields a significantly lower spiked protrusion density than *mKOsn* and *mKOS52A*. **P*<0.05; ****P*<0.001; error bars indicate s.d. Scale bars: 50 μm.

the regulation of Singed by phosphorylation at Ser52 in class III and class IV neurons, we generated phosphomimetic and non-phosphorylatable mutant constructs inserted at the same genomic location to guarantee similar, high levels of expression.

We first addressed whether phosphorylation at Ser52 suppresses Singed activity in class IV neurons. Overexpression of the full-length construct or of the phosphovariant constructs in class IV neurons using *477Gal4* induced the formation of spiked protrusions that contained Singed (Fig. 7B-D,H-J). All three constructs led to a significant shortening and straightening of the terminal branchlets (Fig. 7L,M). In addition, the non-phosphorylatable form led to a prominent induction of high-order branching (number of terminal branchlets, 276±75; control, 131±15; $P<0.001$; non-modified version, 163±15; $P<0.001$) (Fig. 7K). Taken together, overexpression of Singed is sufficient to induce shortening and straightening of the class IV terminal branchlets independently of the phosphorylation state of Singed. However, the difference in the phenotypes obtained provides a first indication that phosphorylation can modulate the control of dendrite branching by Singed.

To further understand the role of phosphorylation, all three constructs were used to rescue the *singed* mutant phenotype in class III neurons (Fig. 7N-Q). Importantly, expression of the phosphomimetic construct resulted in a significantly reduced spiked protrusion density (mKOsnS52D, 0.09±0.01) compared with the other two constructs (mKOsn, 0.13±0.01; mKOsnS52A, 0.12±0.2; $P<0.05$) (Fig. 7P,Q). This lower activity correlated with poor enirchment of the phosphomimetic construct in the terminal branchlets (supplementary material Fig. S7), suggesting a correlation between the Singed phosphorylation status and its localization at the filopodium. Hence, phosphorylation is part of the control mechanism for Singed activity in class III spike formation.

DISCUSSION

We have investigated how the specific morphologies of dendrites of distinct neuronal classes are formed. We provide evidence that the actin regulator fascin (Singed in *Drosophila*) is an important determinant of class III neuron dendrite morphology as it is necessary for the formation of the characteristic terminal branchlets of these neurons. We also show it acts as an effector of the transcription factor Cut. In addition, loss of fascin function induces a partial modification of class III neurons toward class IV neuron morphology, and fascin overexpression in class IV neurons elicits the formation of spiked protrusions typical of class III. This indicates that fascin is a key effector of the distinction between these two neuronal types.

Given the variety of dendritic structures (Fiala et al., 2008), the question arises as to whether a unifying mechanism underlies the formation of all types of branches. The first step in the elaboration of dendrite branches is the formation of a dynamic process, which is often defined as a filopodium mainly on morphological grounds (Hume and Purves, 1981). Subsequent regulation through adhesion molecules and activity defines which subset of filopodia will be maintained and give rise to dendritic branches (Cline and Haas, 2008; Heiman and Shaham, 2010). We questioned whether dendritic filopodia represent distinct structures in different types of neurons and thus carried out a quantitative comparative analysis of class III and class IV da neurons. We show that the dynamic properties, the cytoskeletal organization, the morphology and the molecular composition of filopodia-like terminal branchlets in these two related neurons are distinct. The possibility that distinct mechanisms might be used in different cell types to form filopodia has been discussed previously (Gupton and Gertler, 2007). Indeed, our experiments support the view that the molecular composition of the terminal branchlets can exert a strong influence on their dynamics and morphology. Fascin function is essential for the proper formation of class III terminal branchlets, but it is not required in class IV neurons, which are unaffected by the loss of this unique actin regulator. Taken together, our data suggest a view of filopodia-like terminal branchlets as specialized cellular structures dedicated to the formation of distinct dendrite types.

Remarkably, fascin not only strongly contributes to the morphology of a specific neuronal class, but also helps to define the distinction between two classes of neurons. Similar effects have mainly been ascribed to transcription factors (Crozatier and Vincent, 2008; Grueber et al., 2003a; Hand et al., 2005; Hattori et al., 2007; Jinushi-Nakao et al., 2007; Li et al., 2004; Moore et al., 2002; Parrish et al., 2006; Sugimura et al., 2004). Nonetheless, in class III neurons a change in the specific organization or regulation of the actin cytoskeleton within defined substructures leads to dramatic changes in structural organization toward a class IV-like morphology. Our data thus indicate that molecularly distinct regulation of cytoskeletal function lies at the foundation of type-specific dendritic arborization. Strikingly, they also suggest that the principal traits of specific morphological dendrite patterns can be implemented by utilizing only a small number of primary cytoskeletal regulatory molecules.

How is the specificity of fascin function in class III neurons obtained? We show that fascin is an effector of Cut. Nonetheless, transcriptional regulation of fascin by Cut seems unlikely because Cut is differentially expressed among da neurons (Brewster et al., 2001), whereas fascin is expressed in all da neurons without major differences in expression level at the cell body. An alternative possibility is that Cut controls fascin activation or localization indirectly. Therefore, we addressed the known regulatory control of fascin via phosphorylation and by small GTPases of the Rho family. Whereas the small GTPase Rac1 can activate fascin in mammalian cultured cells (Adams and Schwartz, 2000), we revealed that fascin activity in class III neurons is primarily independent of Rac1. Phosphorylation at Ser39 (Ser52 in *Drosophila*) leads to reduced binding of fascin 1 to actin in vitro (Ono et al., 1997; Yamakita et al., 1996), to reduced formation of fascin-based protrusions in matrix-adherent cells (Adams et al., 1999) and to reduced rescue of invadopodia formation after fascin knockdown in melanoma cells (Li et al., 2010). In mammalian cultured cells, fascin phosphorylation regulates filopodium formation and fascin association to filopodia (Aratyn et al., 2007; Vignjevic et al., 2006). We found that phosphorylation contributes to fascin regulation during class III terminal branchlet formation. A phosphomimetic fascin mutant did not rescue loss of wild-type fascin in class III neurons to the same extent as wild-type fascin, and the reduced function of this construct correlated with its poor enrichment in the terminal branchlets, suggesting an effect of phosphorylation on recruitment. We suggest that the partial effect of Ser52 phosphorylation might reflect the dynamics of class III neuron branchlets, which perhaps do not require prolonged association of fascin with actin bundles (Vignjevic et al., 2006).

Localized recruitment of fascin has been described during the formation of fly bristles (Zhang et al., 2009). Based on our data, we propose a model in which Cut controls a program that results in fascin recruitment to the terminal branchlets of class III neurons, modulated by fascin phosphorylation. In support of this idea, Cut overexpression in class I neurons leads to recruitment of endogenous fascin to the terminal branchlets. Alternative

explanations remain possible. For example, Cut could endow class III neurons with the capacity to respond to extracellular matrix components, which in turn could promote a spatially confined accumulation of fascin (Adams, 1995; Adams et al., 2001).

Taken together, our data clearly show that specific types of dendritic branchlets have distinctive dynamic properties and rely on a defined molecular regulation of the underlying cytoskeleton. Such specificity appears crucial to translate transcriptional neuronal identity codes into morphological shape.

Acknowledgements
We thank F. Payre, S. Plaza and J. Zanet for sharing unpublished data; W. Grueber, Y. N. Jan and T. Suzuki for fly lines; the Bloomington Stock Center, the Developmental Studies Hybridoma Bank and FlyBase for providing reagents and information; A. Tatarnikova, J. Lindner, V. Linne and C. Schuy for experimental support; R. Fässler for access to a spinning disc confocal microscope and S. Wickström for guidance in its use; T. Stradal and R. Klein for insightful discussion; and F. Bradke, K. Rottner, T. Suzuki and V. Linne for critically reading the manuscript.

Funding
G.T. was supported by a Deutsche Forschungsgemeinschaft (DFG) grant [SPP1464, Ta 265/4-1]; funding to A.W.M. and C.D. was via a RIKEN core grant.

Competing interests statement
The authors declare no competing financial interests.

Supplementary material
Supplementary material available online at
http://dev.biologists.org/lookup/suppl/doi:10.1242/dev.077800/-/DC1

References

Adams, J. C. (1995). Formation of stable microspikes containing actin and the 55 kDa actin bundling protein, fascin, is a consequence of cell adhesion to thrombospondin-1: implications for the anti-adhesive activities of thrombospondin-1. *J. Cell Sci.* **108**, 1977-1990.
Adams, J. C. and Schwartz, M. A. (2000). Stimulation of fascin spikes by thrombospondin-1 is mediated by the GTPases Rac and Cdc42. *J. Cell Biol.* **150**, 807-822.
Adams, J. C., Clelland, J. D., Collett, G. D., Matsumura, F., Yamashiro, S. and Zhang, L. (1999). Cell-matrix adhesions differentially regulate fascin phosphorylation. *Mol. Biol. Cell* **10**, 4177-4190.
Adams, J. C., Kureishy, N. and Taylor, A. L. (2001). A role for syndecan-1 in coupling fascin spike formation by thrombospondin-1. *J. Cell Biol.* **152**, 1169-1182.
Andersen, R., Li, Y., Resseguie, M. and Brenman, J. E. (2005). Calcium/calmodulin-dependent protein kinase II alters structural plasticity and cytoskeletal dynamics in Drosophila. *J. Neurosci.* **25**, 8878-8888.
Aratyn, Y. S., Schaus, T. E., Taylor, E. W. and Borisy, G. G. (2007). Intrinsic dynamic behavior of fascin in filopodia. *Mol. Biol. Cell* **18**, 3928-3940.
Bischof, J., Maeda, R. K., Hediger, M., Karch, F. and Basler, K. (2007). An optimized transgenesis system for Drosophila using germ-line-specific phiC31 integrases. *Proc. Natl. Acad. Sci. USA* **104**, 3312-3317.
Branco, T., Clark, B. A. and Häusser, M. (2010). Dendritic discrimination of temporal input sequences in cortical neurons. *Science* **329**, 1671-1675.
Brand, A. H. and Perrimon, N. (1993). Targeted gene expression as a means of altering cell fates and generating dominant phenotypes. *Development* **118**, 401-415.
Brewster, R., Hardiman, K., Deo, M., Khan, S. and Bodmer, R. (2001). The selector gene cut represses a neural cell fate that is specified independently of the Achaete-Scute-Complex and atonal. *Mech. Dev.* **105**, 57-68.
Cant, K., Knowles, B. A., Mooseker, M. S. and Cooley, L. (1994). Drosophila singed, a fascin homolog, is required for actin bundle formation during oogenesis and bristle extension. *J. Cell Biol.* **125**, 369-380.
Cline, H. and Haas, K. (2008). The regulation of dendritic arbor development and plasticity by glutamatergic synaptic input: a review of the synaptotrophic hypothesis. *J. Physiol.* **586**, 1509-1517.
Crozatier, M. and Vincent, A. (2008). Control of multidendritic neuron differentiation in Drosophila: the role of Collier. *Dev. Biol.* **315**, 232-242.
Cuntz, H., Forstner, F., Borst, A. and Häusser, M. (2010). One rule to grow them all: a general theory of neuronal branching and its practical application. *PLoS Comput. Biol.* **6**, e1000877.
Dimitrova, S., Reissaus, A. and Tavosanis, G. (2008). Slit and Robo regulate dendrite branching and elongation of space-filling neurons in Drosophila. *Dev. Biol.* **324**, 18-30.
Faix, J., Breitsprecher, D., Stradal, T. E. and Rottner, K. (2009). Filopodia: complex models for simple rods. *Int. J. Biochem. Cell Biol.* **41**, 1656-1664.
Fiala, J. C., Spacek, J. and Harris, K. M. (2008). Dendrite structure. In *Dendrites* (ed. G. Stuart, N. Spruston and M. Hausser), pp. 1-42. Oxford: Oxford University Press.
Gao, F. B., Brenman, J. E., Jan, L. Y. and Jan, Y. N. (1999). Genes regulating dendritic outgrowth, branching, and routing in Drosophila. *Genes Dev.* **13**, 2549-2561.
Grueber, W. B., Jan, L. Y. and Jan, Y. N. (2002). Tiling of the Drosophila epidermis by multidendritic sensory neurons. *Development* **129**, 2867-2878.
Grueber, W. B., Jan, L. Y. and Jan, Y. N. (2003a). Different levels of the homeodomain protein cut regulate distinct dendrite branching patterns of Drosophila multidendritic neurons. *Cell* **112**, 805-818.
Grueber, W. B., Ye, B., Moore, A. W., Jan, L. Y. and Jan, Y. N. (2003b). Dendrites of distinct classes of Drosophila sensory neurons show different capacities for homotypic repulsion. *Curr. Biol.* **13**, 618-626.
Hand, R., Bortone, D., Mattar, P., Nguyen, L., Heng, J. I., Guerrier, S., Boutt, E., Peters, E., Barnes, A. P., Parras, C. et al. (2005). Phosphorylation of Neurogenin2 specifies the migration properties and the dendritic morphology of pyramidal neurons in the neocortex. *Neuron* **48**, 45-62.
Hashimoto, Y., Parsons, M. and Adams, J. C. (2007). Dual actin-bundling and protein kinase C-binding activities of fascin regulate carcinoma cell migration downstream of Rac and contribute to metastasis. *Mol. Biol. Cell* **18**, 4591-4602.
Hattori, Y., Sugimura, K. and Uemura, T. (2007). Selective expression of Knot/Collier, a transcriptional regulator of the EBF/Olf-1 family, endows the Drosophila sensory system with neuronal class-specific elaborated dendritic patterns. *Genes Cells* **12**, 1011-1022.
Häusser, M., Spruston, N. and Stuart, G. J. (2000). Diversity and dynamics of dendritic signaling. *Science* **290**, 739-744.
Heiman, M. G. and Shaham, S. (2010). Twigs into branches: how a filopodium becomes a dendrite. *Curr. Opin. Neurobiol.* **20**, 86-91.
Holthuis, J. C., Schoonderwoert, V. T. and Martens, G. J. (1994). A vertebrate homolog of the actin-bundling protein fascin. *Biochim. Biophys. Acta* **1219**, 184-188.
Hume, R. I. and Purves, D. (1981). Geometry of neonatal neurones and the regulation of synapse elimination. *Nature* **293**, 469-471.
Hummel, T., Krukkert, K., Roos, J., Davis, G. and Klämbt, C. (2000). Drosophila Futsch/22C10 is a MAP1B-like protein required for dendritic and axonal development. *Neuron* **26**, 357-370.
Jan, Y. N. and Jan, L. Y. (2010). Branching out: mechanisms of dendritic arborization. *Nat. Rev. Neurosci.* **11**, 316-328.
Jinushi-Nakao, S., Arvind, R., Amikura, R., Kinameri, E., Liu, A. W. and Moore, A. W. (2007). Knot/Collier and cut control different aspects of dendrite cytoskeleton and synergize to define final arbor shape. *Neuron* **56**, 963-978.
Lee, T. and Luo, L. (1999). Mosaic analysis with a repressible cell marker for studies of gene function in neuronal morphogenesis. *Neuron* **22**, 451-461.
Lee, A., Li, W., Xu, K., Bogert, B. A., Su, K. and Gao, F. B. (2003). Control of dendritic development by the Drosophila fragile X-related gene involves the small GTPase Rac1. *Development* **130**, 5543-5552.
Li, A., Dawson, J. C., Forero-Vargas, M., Spence, H. J., Yu, X., König, I., Anderson, K. and Machesky, L. M. (2010). The actin-bundling protein fascin stabilizes actin in invadopodia and potentiates protrusive invasion. *Curr. Biol.* **20**, 339-345.
Li, W., Wang, F., Menut, L. and Gao, F. B. (2004). BTB/POZ-zinc finger protein abrupt suppresses dendritic branching in a neuronal subtype-specific and dosage-dependent manner. *Neuron* **43**, 823-834.
Li, W., Li, Y. and Gao, F. B. (2005). Abelson, enabled, and p120 catenin exert distinct effects on dendritic morphogenesis in Drosophila. *Dev. Dyn.* **234**, 512-522.
Luo, L., Liao, Y. J., Jan, L. Y. and Jan, Y. N. (1994). Distinct morphogenetic functions of similar small GTPases: Drosophila Drac1 is involved in axonal outgrowth and myoblast fusion. *Genes Dev.* **8**, 1787-1802.
Mattila, P. K. and Lappalainen, P. (2008). Filopodia: molecular architecture and cellular functions. *Nat. Rev. Mol. Cell Biol.* **9**, 446-454.
Medina, P. M., Swick, L. L., Andersen, R., Blalock, Z. and Brenman, J. E. (2006). A novel forward genetic screen for identifying mutations affecting larval neuronal dendrite development in Drosophila melanogaster. *Genetics* **172**, 2325-2335.
Medina, P. M., Worthen, R. J., Forsberg, L. J. and Brenman, J. E. (2008). The actin-binding protein capulet genetically interacts with the microtubule motor kinesin to maintain neuronal dendrite homeostasis. *PLoS ONE* **3**, e3054.
Meijering, E., Jacob, M., Sarria, J. C., Steiner, P., Hirling, H. and Unser, M. (2004). Design and validation of a tool for neurite tracing and analysis in fluorescence microscopy images. *Cytometry A* **58A**, 167-176.
Moore, A. W., Jan, L. Y. and Jan, Y. N. (2002). hamlet, a binary genetic switch between single- and multiple- dendrite neuron morphology. *Science* **297**, 1355-1358.
Ono, S., Yamakita, Y., Yamashiro, S., Matsudaira, P. T., Gnarra, J. R.,

protein kinase C phosphorylation site on human fascin. *J. Biol. Chem.* **272**, 2527-2533.
Parrish, J. Z., Kim, M. D., Jan, L. Y. and Jan, Y. N. (2006). Genome-wide analyses identify transcription factors required for proper morphogenesis of Drosophila sensory neuron dendrites. *Genes Dev.* **20**, 820-835.
Parsons, M. and Adams, J. C. (2008). Rac regulates the interaction of fascin with protein kinase C in cell migration. *J. Cell Sci.* **121**, 2805-2813.
Paterson, J. and O'Hare, K. (1991). Structure and transcription of the singed locus of Drosophila melanogaster. *Genetics* **129**, 1073-1084.
Roiha, H., Rubin, G. M. and O'Hare, K. (1988). P element insertions and rearrangements at the singed locus of Drosophila melanogaster. *Genetics* **119**, 75-83.
Sholl, D. A. (1953). Dendritic organization in the neurons of the visual and motor cortices of the cat. *J. Anat.* **87**, 387-406.
Sedeh, R. S., Fedorov, A. A., Fedorov, E. V., Ono, S., Matsumura, F., Almo, S. C. and Bathe, M. (2010). Structure, evolutionary conservation, and conformational dynamics of Homo sapiens fascin-1, an F-actin crosslinking protein. *J. Mol. Biol.* **400**, 589-604.
Shepherd, D. and Smith, S. A. (1996). Central projections of persistent larval sensory neurons prefigure adult sensory pathways in the CNS of Drosophila. *Development* **122**, 2375-2384.
Sugimura, K., Yamamoto, M., Niwa, R., Satoh, D., Goto, S., Taniguchi, M., Hayashi, S. and Uemura, T. (2003). Distinct developmental modes and lesion-induced reactions of dendrites of two classes of Drosophila sensory neurons. *J. Neurosci.* **23**, 3752-3760.
Sugimura, K., Satoh, D., Estes, P., Crews, S. and Uemura, T. (2004). Development of morphological diversity of dendrites in Drosophila by the BTB-zinc finger protein abrupt. *Neuron* **43**, 809-822.
Tilney, L. G., Connelly, P. S., Vranich, K. A., Shaw, M. K. and Guild, G. M. (1998). Why are two different cross-linkers necessary for actin bundle formation in vivo and what does each cross-link contribute? *J. Cell Biol.* **143**, 121-133.
Vignjevic, D., Kojima, S., Aratyn, Y., Danciu, O., Svitkina, T. and Borisy, G. G. (2006). Role of fascin in filopodial protrusion. *J. Cell Biol.* **174**, 863-875.
Wulfkuhle, J. D., Petersen, N. S. and Otto, J. J. (1998). Changes in the F-actin cytoskeleton during neurosensory bristle development in Drosophila: the role of singed and forked proteins. *Cell Motil. Cytoskeleton* **40**, 119-132.
Yalgin, C., Karim, M. R. and Moore, A. W. (2011). Immunohistological labeling of microtubules in sensory neuron dendrites, tracheae, and muscles in the Drosophila larva body wall. *J. Vis. Exp.* **10**, 3662.
Yamakita, Y., Ono, S., Matsumura, F. and Yamashiro, S. (1996). Phosphorylation of human fascin inhibits its actin binding and bundling activities. *J. Biol. Chem.* **271**, 12632-12638.
Zanet, J., Stramer, B., Millard, T., Martin, P., Payre, F. and Plaza, S. (2009). Fascin is required for blood cell migration during Drosophila embryogenesis. *Development* **136**, 2557-2565.
Zhang, J., Fonovic, M., Suyama, K., Bogyo, M. and Scott, M. P. (2009). Rab35 controls actin bundling by recruiting fascin as an effector protein. *Science* **325**, 1250-1254.
Zito, K., Parnas, D., Fetter, R. D., Isacoff, E. Y. and Goodman, C. S. (1999). Watching a synapse grow: noninvasive confocal imaging of synaptic growth in Drosophila. *Neuron* **22**, 719-729.